Materials Research Proceedings **32** (2023) 111-118 https://doi.org/10.21741/9781644902615-12

Effects of deformation conditions on the superplastic deformation behavior of LZ91 Mg-Li alloy under electric field

Bao Meng [a*], Feng Pan [b], Jianqiang Yang [c], Dongsheng Li [d], Min Wan [e]

School of Mechanical Engineering and Automation, Beihang University, Beijing, 100191, PR China

[a]mengbao@buaa.edu.cn, [b]buaapanfeng@gmail.com, [c]jianqiangyang@buaa.edu.cn, [d]lidongs@buaa.edu.cn, [e]mwan@buaa.edu.cn

Keywords: Superplastic Deformation Behavior, LZ91 Mg-Li Alloy, Electric Field Assisted

Abstract. The electro-superplastic effect (ESP effect) can enhance the superplastic deformation ability of alloy, and can also make alloy with poor plasticity have superplastic properties. Diverse grain sizes of LZ91 Mg-Li alloy were successfully prepared through equal channel angular pressing (ECAP) process. In order to explore the superplastic deformation behavior of LZ91 Mg-Li alloy under the electric current, an electric field assisted superplastic uniaxial tensile test platform was designed and fabricated. A decreasing constant voltage electrification scheme was proposed, and the experiments under different current densities, initial strain rates and grain sizes were carried out. The results indicate that the true strain-stress curve of LZ91 Mg-Li alloy gradually comes to steady with the increase of current density, presenting a steady-state rheological characteristic. The initial strain rate has a significant effect on the superplastic deformation behavior of LZ91 Mg-Li alloy under high voltage condition. For the fine-grained LZ91 Mg-Li alloy, the electric field can effectively reduce the superplastic deformation temperature and considerably enhance the elongation. This paper enriches the understanding of the superplastic deformation behavior of LZ91 Mg-Li alloy under the action of electric field.

Introduction

Mg-Li alloy is the lightest structural metal, when utilized as a structural material, it can significantly lower the mass of structural parts. The Mg-Li alloy also has the advantages of high specific strength, specific stiffness, excellent damping shock absorption, and good thermal conductivity [1]. The pulsed electric field can decrease the forming temperature of Mg-Li alloy, and reduce its flow stress. Applying an electric field during the superplastic deformation can improve Mg-Li alloy's superplasticity. Therefore, Applying an electric field into the superplastic deformation can enhance the material's superplastic deformation capacity, which is called the ESP effect. The ESP effect can decrease the superplastic deformation temperature and increase its deformation rate, which has attracted considerable scholarly interest domestically and internationally. Li Yao [2] discovered that the elongation and strain rate sensitivity coefficient of Zn-22A1 alloy were significantly enhanced by studying the superplastic properties of Zn-22A1 alloy under the influence of pulse current. Yoshida et al. [3] achieve low-temperature and high-velocity superplastic flow in structural ceramics by employing a reinforced electric field during deformation. They found that the elongation is increased from 5% to 135% after applying 120 V/cm^2 DC to ceramic materials. Wang et al. [4] who successfully welded copper and steel alloys under an external electric field, demonstrated that electric fields can enhance superplasticity.

In this paper, Mg-Li alloy bar with different grain sizes were prepared by equal channel angular pressing (ECAP). In order to investigate the effect of various current densities, initial strain rates, and grain sizes on the mechanical properties of LZ91 Mg-Li alloy, a series of electric field assisted superplastic tensile tests are conducted.

Experimental setup and methodology

Experimental specimen. LZ91 Mg-Li alloy was selected as the experimental material, and the chemical composition is shown in Table 1. The shape and dimensions of the tensile specimen are shown in Fig. 1.

Table 1 Chemical composition of LZ91 Mg-Li alloy (wt.%)

Li	Zn	Mg	Mn	Fe	Cu	Ni	Si
9.21	0.97	base	0.018	0.003	0.0002	0.0003	0.007

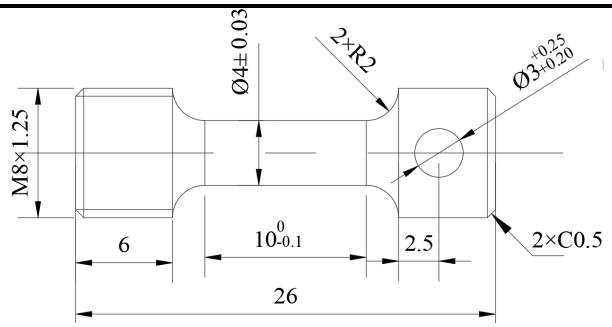

Fig. 1 Tensile specimen dimensions (unit: mm)

Experimental setup. As shown in Fig. 2, The experimental platform consists of an electric field assisted superplastic tensile die, a video extensometer, an infrared thermal imager (FLIR A615), a power supply (SOYI-242000ML), and a fan. The whole set of dies and the cupping machine are connected by a screw thread that holds them together. The power supply is connected to the H59 brass die which has excellent electrical conductivity. The die attached to the cupped machine is made of 45 steel. The insulated material between H59 brass and steel 45 is bake lite.

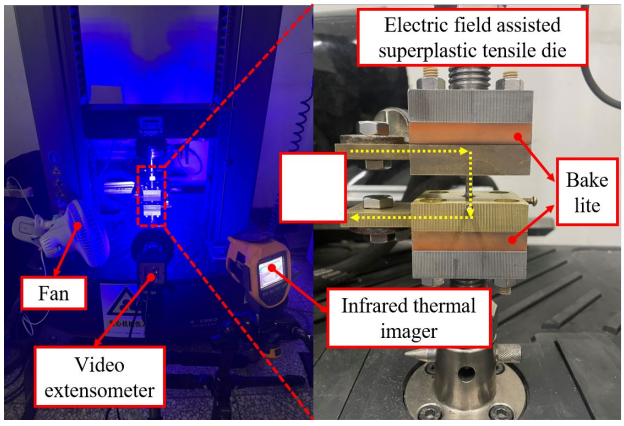

Fig. 2 Electric field assisted superplastic tensile experimental platform

The LZ91 Mg-Li alloy bar was extruded in 0, 4, and 8 passes using ECAP technology to produce specimens with varying grain sizes (β-Li phase) of 18.34, 1.27 and 0.88 μm The B_C path is used to extrude the LZ91 Mg-Li alloy bar in this experiment.

Experimental methodology. During the superplastic deformation process, the relative stability of the specimen temperature is essential. When a constant current is applied to the spacemen, the temperature of the specimen rises rapidly, and it is impossible to maintain a constant temperature. When a constant voltage is applied to the specimen, the rate of temperature rising is reduced compared with the constant current, but the temperature is still not constant. Therefore, a decreasing constant voltage power-on scheme is proposed. The scheme is that power on for a period of time, lower the voltage value and then energized for the same time repeatedly until the specimen is broken.

Materials Research Proceedings **32** (2023) 111-118 https://doi.org/10.21741/9781644902615-12

Results and discussions

The effect of current density on the superplastic deformation behavior of the Mg-Li alloy. The unextruded specimen was installed between the electric field assisted superplastic tensile dies, and five tensile tests were performed at the initial strain rate of 8×10^{-4} s^{-1}. Power-on time was set to 330 s→300 s→300 s→300 s→500 s, and the relevant parameters of the experiments are shown in Table 2. In various experimental situations, the elongation of the specimens is diverse. Thus, the time when the specimen fractures is also different. Table 2 displays the fracture time of each experimental specimen. The current density is constantly changing, so the average value of the current density during the stretching process is used as the reference value for the current density.

Table 2. Experimental parameters of the original specimens

Average current density [A·mm^2]	Power-on settings [V]	Temperature range [°C]	σ_b [MPa]	δ [%]
17.82	2→1.7→1.5→1.3(break)→1.1	165~272	22.35	89
18.53	2.1→1.8→1.6→1.4(break)→1.2	185~285	16.05	102
16.69	2.2→1.9→1.7→1.5→1.3(break)	174~321	19.31	95
20.62	2.3→2.0→1.8→1.6→1.4(break)	190~332	13.11	105
22.39	2.4→2.1→1.9→1.7→1.5(break)	224~377	9.31	105

Note 1: "Break" in the table indicates that the specimen has fractured under this voltage value
Note 2: Tensile strength σ_b and elongation δ

Fig. 3 displays the true stress-strain curves of the specimens under various current densities. In the initial tensile stage, the flow stress of the specimen rises rapidly with increasing strain. Meanwhile, the internal dislocations of the specimen multiply and interact with each other, and dynamic recrystallization within the specimen is substantially weaker than the hardening effect. Thus, the specimen exhibits a more obvious hardening phenomenon [5,6]. After the stress peaks, the impact of dynamic recrystallization and recovery within the specimen is enhanced. Dynamic recrystallization can effectively reduce the dislocation density, and lower the effect of work hardening on the specimen, which gradually decreases the deformation resistance of the specimen and the slope of the true stress-strain curve [7-9].

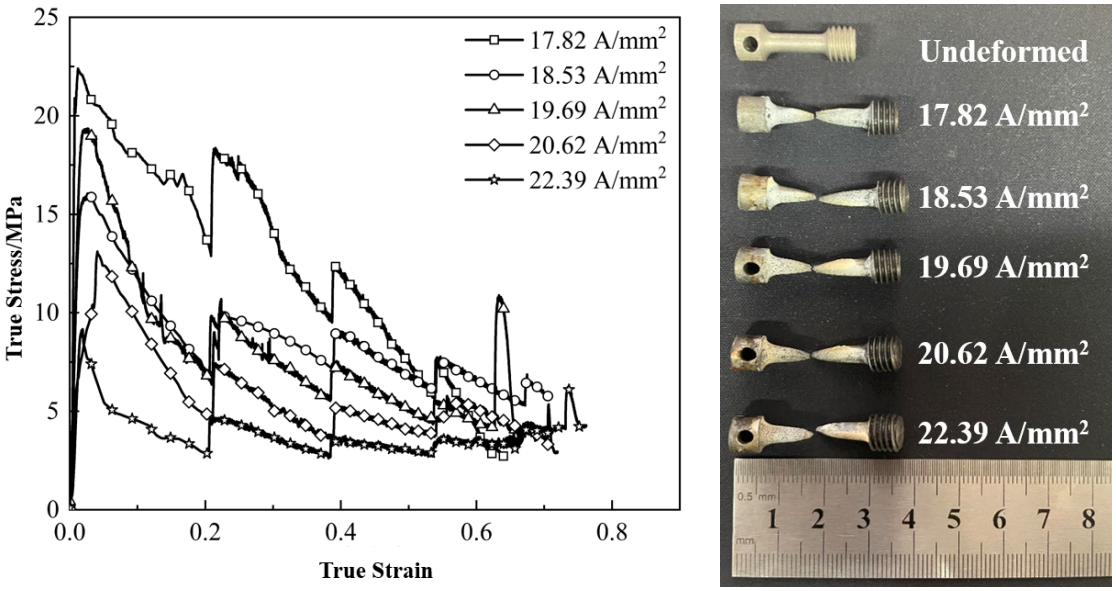

(a) True stress-strain curve (b) Tensile samples

Fig. 3 Experimental results of the initial specimens under different current densities

Materials Research Proceedings **32** (2023) 111-118 https://doi.org/10.21741/9781644902615-12

In Fig. 3, it is evident that all true stress-strain curves are "zigzags". This is because the voltage decreases during the stretching process, and the temperature of specimen will drop abruptly at the moment of voltage conversion, causing the true stress-strain curve to rise at the moment of voltage conversion. Thus, each stress surge represents a change in the voltage value. As the current density goes up, the temperature of the specimen grows as well. When the temperature goes up, the atomic kinetic energy and the activity of dislocations increase. Therefore, the LZ91 Mg-Li is more likely to deform under the action of external forces.

Table 2 displays the tensile strength σ_b and elongation of the original specimen under various energized conditions. Table 2 reveals that, the tensile strength of specimen decreases and the elongation rises as the current density increases. Maximum superplastic elongation is 105% under the current density of 20.62 A/mm^2. As the strain increases, the true stress-strain curve of 20.62 A/mm^2 gradually flattens and exhibits steady-state rheological characteristics. The true stress-strain curve of 22.39 A/mm^2 also showed steady-state rheological characteristics. However, compared to the current density of 20.62 A/mm^2, the elongation of Mg-Li alloy didn't get any better, which meant that the deformation temperature of Mg-Li alloy at a current density of 20.62 A/mm^2 had exceeded the optimal superplastic deformation temperature. The difference of elongation at electric field is not very obvious, and the maximum difference is only 16%, which indicates that the ESP effect has little effect on the elongation. The Joule heating effect generated by the current is still more influential on the elongation of the coarse grain LZ91 Mg-Li alloy.

The effect of initial strain rate on the superplastic deformation behavior of the Mg-Li alloy. The relevant experiment parameters are presented in Table 3. In different strain rate experiments, the magnitude of change in current density is not uniform, so voltage is used as the electric field parameter.

Table 3 Experimental parameters of the original specimens with various initial strain rates

Power-on settings [V]	strain rate [s^{-1}]	Temperature range [°C]	σ_b [MPa]	δ [%]
2.1→1.8→1.6 →1.4→1.2	4×10^{-3}	179~260	29.16	64
	8×10^{-4}	185~285	15.90	105
	4×10^{-4}	167~320	19.71	97
2.2→1.9→1.7 →1.5→1.3	4×10^{-3}	170~258	33.30	70
	8×10^{-4}	174~321	19.22	95
	4×10^{-4}	188~302	10.33	110

Fig. 4 shows the true stress-strain curves under different initial strain rates. As Fig. 4 (a) shows, the curve of 8×10^{-4} $s^{-1}$and 4×10^{-4} s^{-1} are relatively close and show steady-state rheological characteristics at low voltage. This phenomenon indicates that the superplastic deformation behavior of LZ91 Mg-Li alloy is less affected by the initial strain rate at low voltage. However, at high voltage, as shown in Fig. 5, the flow stress of the material decreases significantly as the initial strain rate decreases. This indicates that under high voltage, the initial strain rate has a great influence on the superplastic deformation behavior of the material. Fig. 5 (a) shows the true stress-strain curve with an initial strain rate of 4×10^{-4} s^{-1} "upturns". This is because the deformation temperature is higher, and the grain of Mg-Li alloy continues to get coarser at a low initial strain rate. This slows down the process of grain boundary slippage. At the same time, the internal recovery and dynamic recrystallization of material alternate, significantly reducing the density of dislocations, leading to dislocation plugging and entanglement, which makes the material less likely to deform.

Materials Research Proceedings **32** (2023) 111-118 https://doi.org/10.21741/9781644902615-12

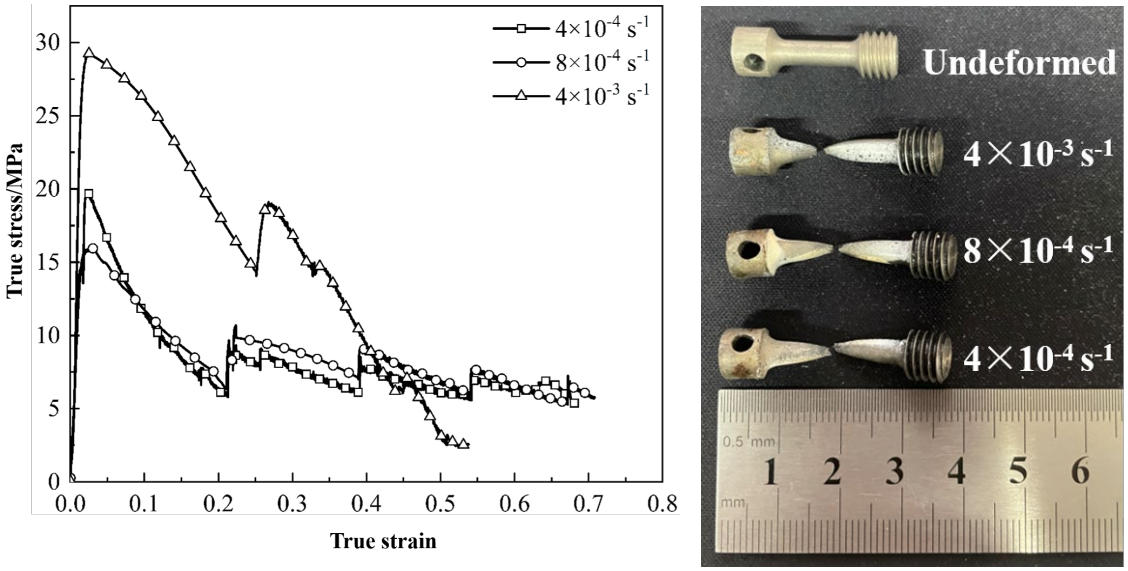

(a) True stress-strain curve (b) Tensile samples

Fig. 4 Experimental results of the initial specimens with different initial strain rates at low voltage

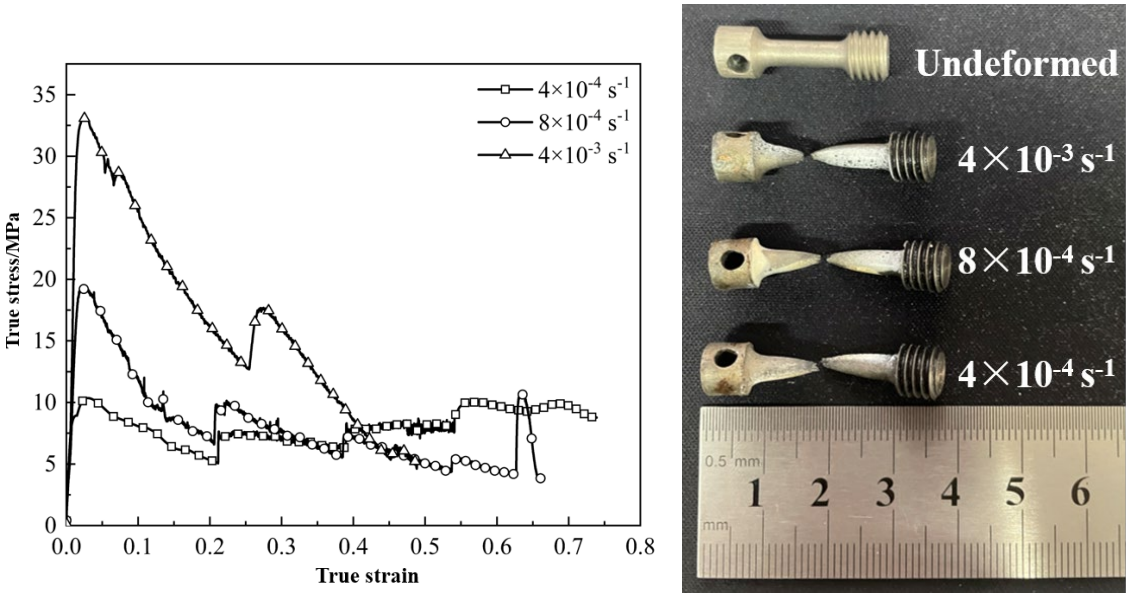

(a) True stress-strain curve (b) Tensile samples

Fig. 5 Experimental results of the initial specimens with different initial strain rates at high voltage

Table 3 lists the tensile strength and elongation of the LZ91 Mg-Li alloy at different initial strain rates. It can be noticed that the tensile strength of Mg-Li alloy declines with the decreasing initial strain rate, which is more obvious at high voltage. When the initial strain rate drops at low voltage, the elongation of Mg-Li alloy increases first and then decreases. The decrease in elongation can be attributed to the fact that a low voltage makes the electro-plasticity effect less apparent. Besides, long-term energization causes high-temperature oxidation of LZ91 Mg-Li alloy. Thus, the material goes into the necking stage early which causes high temperature and cracks in some places. At high voltage, the elongation of Mg-Li alloy increases with the decrease of the initial strain rate, and the maximum elongation of 110% is reached at the initial strain rate

Materials Research Proceedings **32** (2023) 111-118 https://doi.org/10.21741/9781644902615-12

of 4×10^{-4} s^{-1}, which also proves that higher current density is more effective for improving the superplasticity of materials.

The effect of initial grain size on the superplastic deformation behavior of the Mg-Li alloy. Mg-Li alloy with various grain sizes (β-Li phase) of 18.34, 1.27 and 0.88 μm were utilized to conduct the experiments. The average grain size of β-Li phase is the reference value. The relevant parameters of the experiment are shown in Table 4.

Table 4 Experimental parameters of specimens with different grain sizes

Power-on settings [V]	Grain size [μm]	Temperature range [°C]	σ_b [MPa]	δ [%]
2.0→1.7→1.5 →1.3→1.1	18.34	179~260	22.20	89
	1.27	185~285	41.15	115
	0.88	167~320	19.45	130
2.2→1.9→1.7 →1.5→1.3	18.34	170~258	19.17	95
	1.27	174~321	7.12	148
	0.88	188~302	22.34	133

The true stress-true strain curves of LZ91 Mg-Li alloy with different grain sizes are shown in Fig. 6 and Fig. 7. It can be seen that no matter what energization conditions, the flow stress of fine grain LZ91 Mg-Li alloy decreases more obviously, because the refinement of the grain can reduce the superplastic deformation temperature. Thus, at the superplastic deformation temperature appropriate for the initial LZ91 Mg-Li alloy, the recrystallization of the fine grain Mg-Li alloy is more completely and has exceeded the appropriate superplastic deformation temperature. At the same time, it can be seen from the figure that the effect of fine crystal strengthening is obvious.

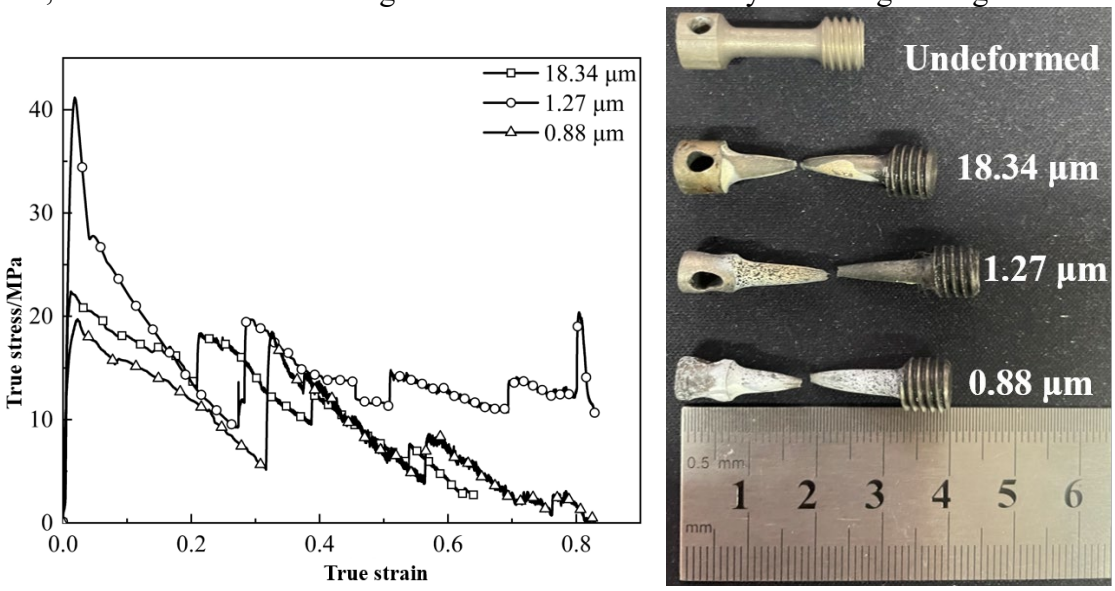

(a) True stress-strain curve (b) Tensile samples

Fig. 6 Experimental results of the specimens with different grain size at low voltage

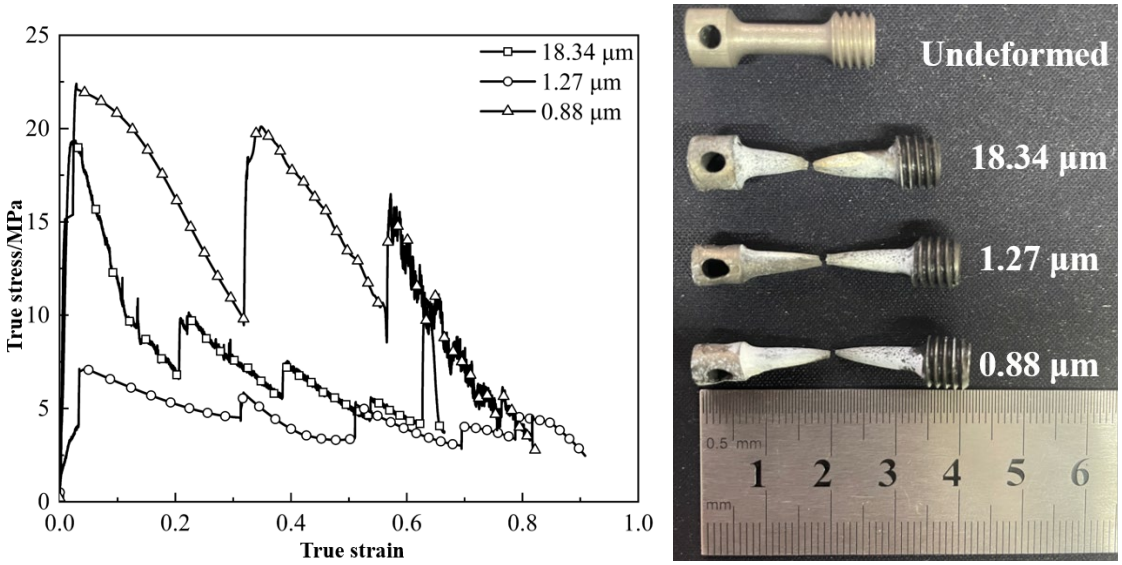

(a) True stress-strain curve (b) Tensile samples

Fig. 7 Experimental results of the specimens with different grain size at high voltage

As shown in Table 4, the elongation of Mg-Li alloy whose grain size (*β*-Li phase) is 1.27 μm reaches 148% under the voltage conditions of 2.2 V→1.9 V→1.7 V→1.5 V→1.3 V, and the true stress-strain curve is basically flat. The superplastic temperature of Mg-Li alloy with initial grain size (*β*-Li phase) of 0.88 μm is low, which indicates that the refinement of the grain can reduce the superplastic temperature of Mg-Li alloy. Therefore, the electric field has a great influence on the elongation on the fine-grained LZ91 Mg-Li alloy.

Conclusions

Through electric field assisted superplastic tensile tests, the effects of current density, initial strain rate, and initial grain size on the superplastic deformation of LZ91 Mg-Li alloy were investigated. The following conclusions can be drawn:

1. The true strain-stress curve of LZ91 Mg-Li alloy gradually comes to steady with the increase of current density, presenting a steady-state rheological characteristic.
2. At low voltage, the initial strain rate has less influence on the superplastic deformation behavior of LZ91 Mg-Li alloy. At high voltage, the elongation of Mg-Li alloy increases as the initial strain rate decreases, reaching a maximum of 110% at an initial strain rate of 4×10^{-4} s^{-1}, and the tendency of true stress-stain curve appears “upturned”.
3. For the fine-grained LZ91 Mg-Li alloy, the electric field can effectively reduce the superplastic deformation temperature and considerably enhance the elongation under the same energized conditions.

References

[1] Jia Y. LZ91 Mg-Li alloy superplastic performance and negative angle box parts superplastic forming [D]. Harbin Institute of Technology, 2017.

[2] Li Yao, Dong Xiao Hua. Dynamic analysis of dislocation activation in electro-plastic effect of Zn-22%A1 alloy, Journal of Jiang Han University (Natural Sciences), 2007 (03): 39-41.

[3] Yoshida H. Sasaki Y. Low temperature and high strain rate superplastic flow in structural ceramics induced by strong electric-field [J]. Scripta Material, 2018, 146: 173-177. https://doi.org/10.1016/j.scriptamat.2017.11.042

[4] Wang Yaoli, Wang Guangxin, Zhang keke. Electro-superplastic solid state welding of 40Cr/QCr0.5[J]. Materials (Basel), 2018, 11 (7). https://doi.org/10.3390/ma11071153

[5] Bi D, Zhang J, Cui H X. Calculation of extrusion force of equal channel corner extrusion die[J]. Heavy Machinery, 2001 (6): 34-36.

[6] Li X F, Cao X D, Wang B, et al. Research progress of Ti alloy electro-assisted plastic forming technology[J]. Aerospace Manufacturing Technology, 2021, 64 (17): 22-30.

[7] Ding X F, Shuang Y H, Lin W L, et al. Rheological behavior and constitutive model of extruded Mg alloy[J]. Chinese Journal of Plastic Engineering, 2017, 24 (06): 165-171.

[8] Gao X B, He C M, Yao T, et al. Dynamic softening behavior and microstructure evolution of Al-Mg-Li alloy[J]. Journal of Specimens and Heat Treatment, 2022, 43 (11): 170-179.

[9] G. D Urso, C. Giardini, M. Quarto, Characterization of surfaces obtained by micro-EDM milling on steel and ceramic components, The International Journal of Advanced Manufacturing Technology, 2018 (97): 2077-2085. https://doi.org/10.1007/s00170-018-1962-5

[10] Pu Y, Kou S, Zhang Z, et al. Effects of return son composition, microstructure and mechanical properties of GH4169 super alloy[J], China Foundry, 2017, 14 (4): 244-250. https://doi.org/10.1007/s41230-017-5125-3

[11] Dong D Y, Liu Y, Wang L, et al. Effect of strain rate on dynamic deformation behavior of DP780 steel laser welded joint[J]. Acta Metallurgica Sinica, 2013 ,49 (12): 1493-1500. https://doi.org/10.3724/SP.J.1037.2013.00341

[12] Liu Y, Wang J, He S S, et al. Effect of long-term aging on dynamic tensile deformation behavior of GH4169 alloy[J]. Acta Metallurgica Sinica, 2012, 48 (1): 49-55. https://doi.org/10.3724/SP.J.1037.2011.00435

[13] Liu Y, Li Z Q, Zhao B, et al. Superplastic deformation behavior and constitutive model of TA32 Ti alloy[J]. Rare Metal Specimens and Engineering, 2022, 51 (10): 3752-3761.

[14] Zhang T Y. Study on low-temperature superplastic deformation of fine-grained TC4 alloy[D]. Central South University, 2014.